Demonstration of Deutsch's Algorithm on a Stable Linear-Optical Quantum Computer

Pei Zhang,[1a] Rui-Feng Liu,[1] Yun-Feng Huang,[2] Hong Gao,[1] and Fu-Li Li[1]
[1] *MOE Key Laboratory for Nonequilibrium Synthesis and Modulation of Condensed Matter, Department of Applied Physics, Xi'an Jiaotong University, Xi'an 710049, People's Republic of China*
[2] *Key Laboratory of Quantum Information, University of Science and Technology of China, CAS, Hefei 230026, People's Republic of China*

We report an experimental demonstration of quantum Deutsch's algorithm by using linear-optical system. By employing photon's polarization and spatial modes, we implement all balanced and constant functions for quantum computer. The experimental system is very stable and the experimental data are excellent in accordance with the theoretical results.

PACS numbers: 03.67.Lx, 03.67.Mn, 42.50.Dv

[a] zhang.pei@stu.xjtu.edu.cn

I. INTRODUCTION

Quantum computation may solve some complex computational problems and hit the security of the classical cryptography. It has attracted much interest to investigate quantum algorithm and to realize quantum hardware, which are very important to quantum information processing and quantum computation. The ideas of quantum processors and computers have been experimented in many physical systems, including ion traps [1], nuclear spins in magnetic resonance [2], super-conducting resonators [3], semiconductor quantum dots [4], neutral atoms [5], and linear optics [6–8]. In linear optical system, it is easy to deal with entanglement and decoherence, and the incorporation of detection and post-selection make it possible to achieve all-optical quantum computers [9]. So linear optical system is a good candidate for implementing quantum algorithms [10, 11]. The system of single-photon few-qubit has been used to build the deterministic quantum information processor (QIP). And the few-qubit QIPs have drawn much attention for the applications in quantum optics and quantum computation [12–18]. Especially, the implementation of single-photon two-qubit (SPTQ) controlled-NOT (CNOT) gate has been reported by Fiorentino et al. [18]. This robust CNOT gate can be utilized to perform a variety of quantum logic operations that are necessary for SPTQ and opens a way to the implementation of SPTQ protocols for few-qubit QIP. In this context, by using this robust CNOT gate and the SPTQ state, we experimentally demonstrate the Deutsch's algorithm.

The first quantum algorithm was proposed by Deutsch in 1985 [19], then extended by Deutsch and Jozsa in 1992 [20]. Deutsch's algorithm combines quantum parallelism with a property of quantum interference. The problem which is solved in Deutsch's algorithm can be described as follow. Suppose we are given a boolean function $f(x)$ where x is either 0 or 1. Note that there are only four possible results of this sort: $f(x) = 0$, $f(x) = 1$, $f(x) = x$, and $f(x) = inv(x)$ ('inv' is the inversion operation). Suppose that we do not want to know exactly which of the four functions $f(x)$ is; rather all we want to know is whether $f(x)$ is a constant function or a balanced function, where constant function means $f(0) = f(1)$ and balanced function means $f(0) \neq f(1)$. With classical computation, we can of course simply compute $f(x)$ on both inputs 0 and 1, then judge which it is. But that takes two separate computations. What Deutsch discovered is that, if $f(x)$ is represented by a system of qubits, it is possible to manipulate the system so that all the needed computations can be done in parallel, and when a measurement is made at the end, the results will reveal whether $f(x)$ is balanced or constant, even though it will not reveal preciously which function $f(x)$ is. Due to Deutsch's algorithm, we can find a separation between what a classical computer and a quantum computer can achieve, that is, the classical computer has to run the $f(x)$ twice to distinguish a balanced function from a constant function while a quantum computer does the job just in one go.

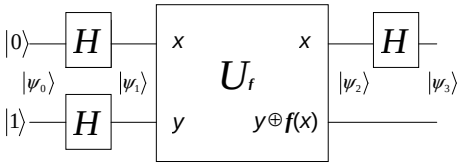

FIG. 1. Quantum circuit of Deutsch's algorithm. H is the Hadamard gate.

Fig. 1 is the quantum circuit implementing Deutsch's algorithm [21]. U_f is the quantum operation which takes inputs $|x, y\rangle$ to $|x, y \oplus f(x)\rangle$. A brief explanation is given below. We start with two qubits, one in state $|0\rangle$ and the other in state $|1\rangle$. The Hadamard gate is used to prepare the first qubit in the superposition state $(|0\rangle + |1\rangle)/\sqrt{2}$ and the other in $(|0\rangle - |1\rangle)/\sqrt{2}$. After the Hadamard transformation,

$$|\Psi_1\rangle = \hat{H}\,|\Psi_0\rangle = (|0\rangle + |1\rangle)(|0\rangle - |1\rangle)/2. \tag{1}$$

Applying U_f to $|\Psi_1\rangle$, we obtain $|\Psi_2\rangle$ to be one of two possible states depending on $f(x)$:

$$|\Psi_2\rangle = \begin{cases} \pm \begin{bmatrix} \frac{|0\rangle+|1\rangle}{\sqrt{2}} \end{bmatrix} \begin{bmatrix} \frac{|0\rangle-|1\rangle}{\sqrt{2}} \end{bmatrix}, & f(0) = f(1), \\ \pm \begin{bmatrix} \frac{|0\rangle-|1\rangle}{\sqrt{2}} \end{bmatrix} \begin{bmatrix} \frac{|0\rangle-|1\rangle}{\sqrt{2}} \end{bmatrix}, & f(0) \neq f(1). \end{cases} \tag{2}$$

The final Hadamard gate is applied on the first qubit,

$$|\Psi_3\rangle = \begin{cases} \pm\,|0\rangle \begin{bmatrix} \frac{|0\rangle-|1\rangle}{\sqrt{2}} \end{bmatrix}, & f(0) = f(1), \\ \pm\,|1\rangle \begin{bmatrix} \frac{|0\rangle-|1\rangle}{\sqrt{2}} \end{bmatrix}, & f(0) \neq f(1). \end{cases} \tag{3}$$

So we can determine $f(x)$ to be balanced or constant by only measuring the first qubit once.

TABLE I. Four different cases of Deutsch's algorithm

Class	**Function**	**Operation**	U_f
Constant	$f(x) = 0$	$\|x, y\rangle \to \|x, y \oplus 0\rangle$	*I (Identity)*
Constant	$f(x) = 1$	$\|x, y\rangle \to \|x, y \oplus 1\rangle$	NOT
Balanced	$f(x) = x$	$\|x, y\rangle \to \|x, y \oplus x\rangle$	CNOT
Balanced	$f(x) = inv(x)$	$\|x, y\rangle \to \|x, y \oplus (x \oplus 1)\rangle$	Z-CNOT

II. IMPLEMENTING OF CNOT GATE

From the above description, to physically test the algorithm, we need a device which can implement the U_f operations for the four possible functions. All the possible $f(x)$ functions and U_f operations are summarized in Table I. So the realizations of four different U_f operations are the main works for testing Deutsch's algorithm. In the first case of $U_f = I$. It means that the second qubit never changes whatever the first qubit being 0 or 1. So this can be recognized as an *Identity* operation to the two qubits. The second case shows that U_f is a NOT gate. The second qubit always flips no matter what the first qubit is. In the third case, U_f is a CNOT gate. The second qubit flips when the first qubit is 1. While in the last case, U_f is a zero-controlled-NOT (Z-CNOT) gate, where the second qubit flips when the first qubit is 0. For these four different U_f operations, *Identity* operation and NOT operation are very simple to be realized; and the Z-CNOT gate can be obtained from CNOT gate with some small changes. So CNOT gate is the fundamental and essential part to execute the Deutsch's algorithm. In this context, we start with a CNOT gate realized by employing polarization and spatial positions of photons [18], construct the four different gates and U_f operations, and carry out the Deutsch's algorithm.

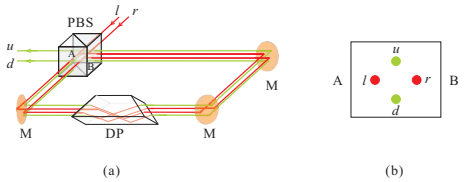

FIG. 2. (a) is the optical implementation of CNOT gate by employing polarization and spatial positions of photons. Dove prism (DP) is inclined at 45°. Red lines show the left (l) and right (r) spatial modes, and green lines show the up (u) and down (d) spatial modes; (b) shows the spatial positions of input and output beams on the splitting plane AB of polarized beam splitter (PBS).

The CNOT gate is shown in Fig. 2. Dove prism (DP) is inclined at 45° angle relative to the horizontal plane (showing in Fig. 2(a)), so the images which pass through it from left to right will be rotated by 90°. Suppose the polarized beam splitter (PBS) here transmits vertical-polarized (V) photons and reflects horizontal-polarized (H) ones. So the V photons travel counterclockwise while the H photons travel clockwise. With a DP inclined at 45°, the spatial mode of V (H) photons oriented 90° (−90°). Specifically, the left-right (l-r) section of the input photons are rotated into the up-down (d-u) section of the output beam for V photons but into the u-d section for H photons (showing in Fig. 2(b)). If we define photon's polarization as the control qubit ($H \to 0$ and $V \to 1$) and spatial mode as the target qubit ($l\&u \to 0$ and $r\&d \to 1$), the CNOT operation can be described as follow:

$$|H\rangle|l\rangle \Longrightarrow |H\rangle|u\rangle, \qquad |H\rangle|r\rangle \Longrightarrow |H\rangle|d\rangle, \qquad |V\rangle|l\rangle \Longrightarrow |V\rangle|d\rangle, \qquad |V\rangle|r\rangle \Longrightarrow |V\rangle|u\rangle. \tag{4}$$

The CNOT gate of Fig. 2 is a polarization Sagnac interferometer, and the two counter-propagating photons always undergo the same amount of phase disturbance. So this optical CNOT gate is with an inherent stability which requires no active stabilization.

III. EXPERIMENT AND RESULTS

We experimentally realize the Deutsch's algorithm by using the CNOT gate mentioned above. The experimental setup is shown in Fig. 3. We use a He-Ne laser (MELLES GRIOT, 05-LHP-171) with deep attenuation as the single photon source (about 150,000 counts per second). All the PBS are quasi-symmetric and transmit V photons while reflect H photons. Polarizer and half wave-plate (HWP_1) are used to prepare photon's polarization states. Here we

prepare the initial polarization of photons as H. 50% beam splitter (BS) and a mirror (M) are used to prepare the photon's spatial-mode states. The piezo-transmitter (PZT) on the first mirror is used to control the relative phase φ between two spatial modes. HWP_2 and HWP_3 at 22.5° are used as the polarization Hadamard gates. The state after HWP_2 can be written as:

$$|\psi_1\rangle = \left[\frac{|H\rangle + |V\rangle}{\sqrt{2}}\right]\left[\frac{|l\rangle + e^{i\varphi}|r\rangle}{\sqrt{2}}\right]. \tag{5}$$

Especially when $\varphi = \pi$, $|\psi_1\rangle$ is equal to $|\Psi_1\rangle$ which is mentioned above. So this single-photon two-qubit state can be used as the input state of Deutsch's algorithm as we described in Fig. 1. Then this state will be evolved by the U_f operation. The detection part consists of a Hadamard gate (HWP_3), PBS_2 and two single photon detectors (D_1 and D_2). Exactly, the detection is a projective measurement on photon's polarization state, known as the target qubit state, which is similar to the Deutsch's algorithm.

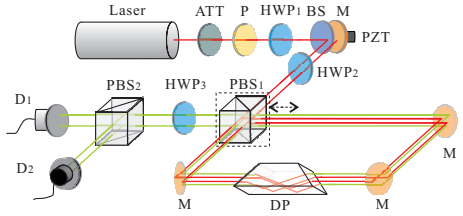

FIG. 3. Experimental setup of Deutsch's algorithm. The source is a He-Ne laser (MELLES GRIOT, 05-LHP-171) of wavelength 632.8 nm. We attenuate the coherent light into single photon level by using some neutral attenuators denoted by ATT. P denotes the polarizer for initial states preparation. Three half wave-plates (HWP) and two polarized beam splitters (PBS) are used in setup. A PZT actuator is used to modulate the phase φ between l and r pathes. Dove plate (DP) is set at 45°. Detectors (D_1 and D_2) are single photon counting modules (SPCM-AQRH-14-FC). All the mirrors are marked as M.

The key point to carry out the Deutsch's algorithm is how to realize the four different cases of U_f operation. We will discuss these four U_f operations below.

Constant function $f(x)$: In the constant function case, U_f can be *Identity* or NOT operation. For *Identity* operation, we can simply remove PBS_1 in our setup and set DP at −45°. Therefore, photons in l or r will always undergo a counter-clockwise route and be outputted in u or d respectively, without the effect of polarization. This means that the target qubit (spatial mode of photons) will not change with control qubit (polarization of photons). We can deduce the process as follow:

$$\begin{aligned} |\psi_1\rangle \xrightarrow{I} |\psi_2\rangle &= \left[\frac{|H\rangle + |V\rangle}{\sqrt{2}}\right]\left[\frac{|u\rangle + e^{i\varphi}|d\rangle}{\sqrt{2}}\right] \\ \xrightarrow{HWP_3} |\psi_3\rangle &= |H\rangle\,\frac{|u\rangle + e^{i\varphi}|d\rangle}{\sqrt{2}}. \end{aligned} \tag{6}$$

While for the NOT operation, we can remove PBS_1 in our setup and set DP at 45°. Then $|l\rangle$ is converted to $|u\rangle$ and $|r\rangle$ is converted to $|d\rangle$. Applying a Hadamard gate (HWP3), we can obtain

$$\begin{aligned} |\psi_1\rangle \xrightarrow{NOT} |\psi_2\rangle &= \left[\frac{|H\rangle + |V\rangle}{\sqrt{2}}\right]\left[\frac{|d\rangle + e^{i\varphi}|u\rangle}{\sqrt{2}}\right] \\ \xrightarrow{HWP_3} |\psi_3\rangle &= |H\rangle\,\frac{|d\rangle + e^{i\varphi}|u\rangle}{\sqrt{2}}. \end{aligned} \tag{7}$$

For the above two cases, we can only detect the polarization qubits, the results are same and without any changes when we adjust the relating phase φ. So, in our setup, when the boolean function $f(x)$ is a constant function, the detector D_2 will be clicked and no photons arrive at D_1. Fig. 4(a) shows our experimental results of $U_f = I$, and Fig. 4(b) shows the results of $U_f = NOT$. Because there is no interference in these processes, the counts of D_1 and D_2 do not change while modulating the voltage of PZT. We can see that our experimental results are very well fitted to the theoretical analysis above.

Balanced function $f(x)$: In this case, $f(x) = x$ or $f(x) = inv(x)$. We need to place the PBS_1 into our the optical route. So the H photons and V photons will travel through the DP in different directions. As we have discussed above, when we set the DP at 45° (−45°), this will be the CNOT (Z-CNOT) gate for the input state $|\psi_1\rangle$ shown in

Eq. (5). Using the corresponding relations of Eq. (4), the theoretical analysis of $U_f = CNOT$ is shown below.

$$|\psi_1\rangle \xrightarrow{CNOT} |\psi_2\rangle = \frac{1}{2}(|H\rangle|u\rangle + e^{i\varphi}|H\rangle|d\rangle + |V\rangle|d\rangle + e^{i\varphi}|V\rangle|u\rangle)$$
$$\xrightarrow{HWP_3} |\psi_3\rangle = \frac{1}{2\sqrt{2}}[(1+e^{i\varphi})|H\rangle(|u\rangle+|d\rangle) + (1-e^{i\varphi})|V\rangle(|u\rangle-|d\rangle)]. \quad (8)$$

For Z-CONT operation, we set the DP at $-45°$. The output state is

$$|\psi_3\rangle = \frac{1}{2\sqrt{2}}[(1+e^{i\varphi})|H\rangle(|u\rangle+|d\rangle) - (1-e^{i\varphi})|V\rangle(|u\rangle-|d\rangle)]. \quad (9)$$

For these two operations, we still detect the polarization qubits. Then we can get two curves which show the photon counts of two detectors changing with the relative phase between two spatial modes. Fig 4(c) corresponds to CNOT operation and Fig. 4(d) corresponds to Z-CNOT operation. From Eq. (8) and Eq. (9), we know that the theoretical results are sinusoidal functions. And our experimental data fit them well.

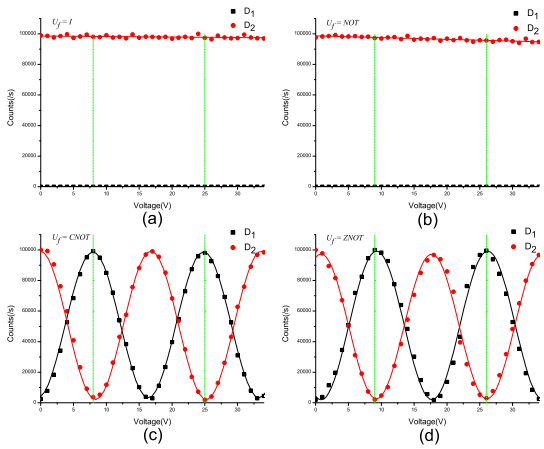

FIG. 4. Experimental data of Deutsch's algorithm. Black square dots show the photon counts of D_1 and red round dots show the photon counts of D_2. Fitting lines are also shown in the figures. The dashed vertical lines mark the proper phases of input state (voltages) of Deutsch's algorithm. By modulating the voltage of PZT from 0 V to 34 V and every 1 V as a step, we record the photon counts of D_1 and D_2 simultaneously. (a) Identity operation of U_f for constant function $f(x) = 0$; (b) NOT operation of U_f for constant function $f(x) = 1$; (c) CNOT operation of U_f for balanced function $f(x) = x$; (d) Z-CNOT operation of U_f for balanced function $f(x) = inv(x)$. Green lines are used to mark the proper points (phases) of the initial states required by Deutsch's algorithm.

Our experimental results are shown in the Fig. 4. In our experiment, we make the relative phase φ adjustable by using a PZT controller. So the output state $|\psi_3\rangle$ contains the phase parameter φ. When we using a PBS for the projective detection, the detector of D_1 and D_2 detect photons of different polarization, V on D_1 and H on D_2. From the Eq. (8) and Eq. (9), we can see that the photon counts of D_1 and D_2 will sinusoidally vary with the φ being continuously changed. We set the phase range for two periods (the voltage of PZT is adjusted from 0 to 34 V) and plot the counts-voltage curves. To the description of Deutsch's algorithm, the input state is a certain state with certain phase (Eq. 1). However, we can get this state simply by setting the phase $\varphi = (2N+1)\pi$ (adjust the PZT in proper voltages), where N is integer. Then, Eq. (8) and Eq. (9) are changed into

$$|\psi_2\rangle_\pi = \pm\frac{1}{2}(|H\rangle - |V\rangle)(|u\rangle - |d\rangle); \quad (10)$$

$$|\psi_3\rangle_\pi = \pm\frac{1}{\sqrt{2}}|V\rangle(|u\rangle - |d\rangle), \quad (11)$$

where '+' is for the CNOT operation and '−' for the Z-CNOT operation. And if we also set the $\varphi = (2N+1)\pi$ in Eq. (6) and Eq. (7), we get

$$|\psi_2\rangle_\pi = \pm\frac{1}{2}(|H\rangle + |V\rangle)(|u\rangle - |d\rangle); \quad (12)$$

$$|\psi_3\rangle_\pi = \pm\frac{1}{\sqrt{2}}|H\rangle(|u\rangle - |d\rangle), \quad (13)$$

where '+' is for the NOT operation and '−' for the I operation. These results are same as $|\Psi_2\rangle$ and $|\Psi_3\rangle$ described in Eq. (2) and Eq. (3). These proper points for Deutsch's algorithm are marked by green lines shown in the Fig 4. From these points, we can claim that it is a constant function when D_1 clicked and a balanced function when D_2 clicked.

Benefit from the Sagnac interferometer, our experimental setup is very stable without any other additional feedback control. This long-time stability makes it possible to change the voltage 1 V as a step from 0 to 32 V. We can define $\eta = |\frac{C_{D1}-C_{D2}}{C_{D1}+C_{D2}}|$ as a contrast ratio to describe the precision of our results, where C_{D1} and C_{D2} denote to the photon counts of D_1 and D_2. Theoretically, the contrast ratio η equal to 1. In our experiment, for the constant functions, $\eta_c = 99.96 \pm 0.03\%$ in Fig. 4(a) and $\eta_c = 99.96 \pm 0.03\%$ in Fig. 4(b); for the balanced functions, the contrast ratio η equals to the interference visibility, in Fig. 4(c), $\eta_b = 95.76 \pm 0.07\%$, and in Fig. 4(c), $\eta_b = 96.13 \pm 0.07\%$. From Fig. 4(a) and 4(b), we can see that the photon counts of D_2 fall with the voltage increasing. This phenomenon is mainly caused by the coupling of multi-mode fiber used in the detection part. We modulate the phase by changing the angle of the first mirror (change the voltage of PZT). Although the change of the angle is very tiny, it will also affect the coupling efficiency turning to worse when photons pass though the setup. Our experimental errors mainly cause by the imperfect of PBS and HWP, the interference visibility, and the effect of DP [22, 23]. However, these errors can be reduced with the improvement of experimental technique.

IV. CONCLUSION

In conclusion, we have experimentally realized the Deutsch's algorithm by using linear optical components. We can determine a property of a function in one evaluation in quantum case instead of two in classical case. When phase φ is zero, we need only a single photon as the input to judge the function $f(x)$: constant function when photons are in H polarization while balanced function when photons are in V polarization. Oliveira et al. have experimentally demonstrated the Deutsch's algorithm with linear-optical components by employing the polarization and transverse spatial mode of photons as qubit [7]. Compared with it, our experimental setup is more robust because the CNOT which we use is a polarization Sagnac interferometer with high stability. We believe these can be used to perform more complex entangled states or few-qubit quantum computation.

V. ACKNOWLEDGEMENT

The authors thank B.-H. Liu for helpful discussion, and acknowledge the National Fundamental Research Program (2010CB923102), National Natural Science Foundation of China (Grant No. 60778021, 10674106 and 10774117) for supporting this work.

[1] J. I. Cirac and P. Zoller, Phys. Rev. Lett. **74**, 4091 (1995).
[2] N. A. Gershenfeld and I. L. Chuang, Science **275**, 350 (1997).
[3] Y. Nakamura, Yu. A. Pashkin, and J. S. Tsai, Nature (London) **398**, 786 (1999).
[4] T. Hayashi, T. Fujisawa, H. D. Cheong, Y. H. Jeong, and Y. Hirayama, Phys. Rev. Lett. **91**, 226804 (2003).
[5] D. Jaksch, Contemp. Phys. **45**, 367 (2004).
[6] M. Mohseni, J. S. Lundeen, K. J. Resch, and A. M. Steinberg, Phys. Rev. Lett. textbf91, 187903 (2003).
[7] A. N. de Oliveira, S. P. Walborn, and C. H. Monken, J. Opt. B: Quantum Semiclass. Opt. **7**, 288-292 (2005).
[8] M. S. Tame, R. Prevedel, M. Paternotro, P. Böhi, M. S. Kim, and A. Zeilinger, Phys. Rev. Lett. **98**, 140501 (2007).
[9] E. Knill, R. Laflamme, and G. Milburn, Nature (London) **409**, 46 (2001).
[10] J. Ahn, T. C. Weinacht, and P. H. Bucksbaum, Science **287**, 463 (2000).
[11] N. Bhattacharya, H. B. van Linden van den Heuvell, and R. J. Spreeuw, Phys. Rev. Lett. **88**, 137901 (2002).
[12] Y. Mitsumori, J. A. Vaccaro, S.M. Barnett, E. Andersson, A. Hasegawa, M. Takeoka, and M. Sasaki, Phys. Rev. Lett. **91**, 217902 (2003).
[13] Z.-B. Chen, J.-W. Pan, Y.-D. Zhang, C. Brukner, and A. Zeilinger, Phys. Rev. Lett. **90**, 160408 (2003).
[14] S. P.Walborn, S. Padua, and C. H. Monken, Phys. Rev. A **68**, 042313 (2003).
[15] M. Genovese and C. Novero, Eur. Phys. J. D **21**, 109 (2002).
[16] K.-Y. Chen, T. Hogg, and R. Beausoleil, Quant. Info. Proc. **1**, 449 (2003).
[17] Y.-H. Kim, Phys. Rev. A **67**, 040301(R) (2003).
[18] M. Fiorentino and F. N. C. Wong, Phys. Rev. Lett. **93**, 070502 (2004).
[19] D. Deutsch, Proc. R. Soc. A **400**, 97 (1985).
[20] D. Deutsch, and R. Josa, Proc. R. Soc. A **439**, 553 (1992).

[21] M. A. Nielsen and I. L. Chuang, Quantum Computation and Quantum Information (Cambridge University Press, Cambridge, 2000).
[22] M. J. Padgett and J. P. Lesso, J. Mod. Optic **46** 175-179 (1998).
[23] I. Moreno, G. Paez, and M. Strojnik, Opt. Commun. **220** 257-268 (2003).